

10<sup>th</sup> International Conference on Solid State Chemistry, Pardubice, Czech Republic

## Defects and charge compensation in CdSiO<sub>3</sub>: A DFT and synchrotron study

Hermi F. Brito<sup>a</sup>, Maria C.F.C. Felinto<sup>b</sup>, Jorma Hölsä<sup>a,c,d</sup>, Taneli Laamanen<sup>c,d,\*</sup>,  
Mika Lastusaari<sup>c,d</sup>, Pavel Novák<sup>e</sup>, Luiz A.O. Nunes<sup>f</sup>, Lucas C.V. Rodrigues<sup>a,c</sup>

<sup>a</sup>Universidade de São Paulo, Instituto de Química, São Paulo-SP, Brazil

<sup>b</sup>Instituto de Pesquisas Energéticas e Nucleares, CQMA, São Paulo-SP, Brazil

<sup>c</sup>University of Turku, Department of Chemistry, FI-20014 Turku, Finland

<sup>d</sup>Turku University Centre for Materials and Surfaces (MatSurf), Turku, Finland

<sup>e</sup>Academy of Sciences of the Czech Republic, Institute of Physics, CZ-16253 Prague 6, Czech Republic

<sup>f</sup>Universidade de São Paulo, Instituto de Física de São Carlos, São Carlos-SP, Brazil

---

### Abstract

The charge compensation effects induced by aliovalent doping were studied in the monoclinic CdSiO<sub>3</sub>. An interstitial oxide ion may be feasible in this host to provide the extra negative charge required by the R<sup>3+</sup> doping. The oxide was studied in CdSiO<sub>3</sub> using density functional theory (DFT) calculations and synchrotron radiation (SR) luminescence spectroscopy. The crystal structure of this host was significantly modified by the interstitial oxide. The experimental band gap energy (E<sub>g</sub>) was perfectly reproduced by the calculations and intrinsic electron traps were revealed. Defect levels were found also in the interstitial oxide containing host, however their role has to be studied further.

© 2013 The Authors. Published by Elsevier B.V.

Selection and/or peer-review under responsibility of the Organisation of the 10th International Conference on Solid State Chemistry.

*Keywords:* cadmium metasilicate; interstitial defect; persistent luminescence; density functional theory calculations

---

### 1. Introduction

The luminescent materials usually consist of an inorganic host material which is activated by a low amount of dopant ions. Isovalent doping is usually used to avoid the creation of structural defects which

---

\* Corresponding author (T. Laamanen). Tel.: +358-2-3336731; fax: +358-2-3336700.

E-mail address: [taanla@utu.fi](mailto:taanla@utu.fi).

can lower the efficiency of conventional luminescence. Aliovalent doping is employed especially in persistent luminescence materials where defects can act as energy storing traps. These materials can store energy when exposed to solar radiation or artificial lighting for minutes or only seconds and release it as light over a period of several hours [1]. This phenomenon arises from the efficient trapping of charge carriers and the slow bleaching of the traps by thermal energy available at room temperature [2].

Aliovalent doping is utilized in the aluminate and silicate based persistent luminescence materials (e.g.  $\text{Sr}_4\text{Al}_{14}\text{O}_{25}:\text{Eu}^{2+},\text{Dy}^{3+}$  [3] and  $\text{Sr}_2\text{MgSi}_2\text{O}_7:\text{Eu}^{2+},\text{Dy}^{3+}$  [4]) where the europium activator is introduced in its trivalent form and reduced to a divalent ion later ( $\text{Dy}^{3+}$  remains trivalent). In the  $\text{CdSiO}_3:\text{R}^{3+}$  materials [5], a trivalent rare earth ion is easily introduced at a divalent Cd site ( $\text{R}_{\text{Cd}}^{\bullet}$  with a single positive net charge in the Kröger-Vink notation [6]) due to the rather similar sizes of these ions [7]. Extra negative charge is thus needed for the charge compensation and the stability of this charge has to be studied. The charge compensation may be provided in  $\text{CdSiO}_3$  by an interstitial oxide ion or a cadmium vacancy (both compensate for two  $\text{R}_{\text{Cd}}^{\bullet}$ ). This host offers an excellent possibility to introduce the interstitial oxide due to the empty space in the structure. Therefore, the effect of this defect on the crystal structure, host band structure and luminescence of the host can be studied. Only the triclinic form of  $\text{CdSiO}_3$  without any defects has so far been studied using theoretical modelling [8] due to its smaller unit cell size. That approach simplifies the calculations but decreases their reliability since persistent luminescence is observed from  $\text{CdSiO}_3$  with a monoclinic structure [5,9].

The goal of this work was to clarify the feasibility of the interstitial oxide ion and its role in the monoclinic  $\text{CdSiO}_3$  through a systematic study of the crystal and electronic structure of this material. *Ab initio* density functional theory (DFT) calculations were combined with experimental synchrotron radiation (SR) spectroscopy. Modifications in the crystal structure due to the introduction of an interstitial oxide were explored using DFT. Structure of the valence (VB) and conduction band (CB) as well as the band gap energy ( $E_g$ ) of the pure and oxide containing host was studied. The defect energy levels in the host band structure were determined, too. The  $E_g$  value was confirmed using the SR UV-VUV spectroscopy. The origin and role of electron and hole traps are discussed based on these results.

## 2. Materials and methods

### 2.1. Materials preparation

The polycrystalline  $\text{CdSiO}_3$  material was prepared with a conventional solid state reaction. Stoichiometric amounts of cadmium acetate ( $\text{Cd}(\text{CH}_3\text{COO})_2 \cdot 2\text{H}_2\text{O}$ , purity: 99 %, Vetec) and fumed silica ( $\text{SiO}_2$ , 99 %, Rhodia) were ground intimately. The mixture was then heated in air at 950 °C for seven hours in an aluminosilicate crucible. Utilization of air can easily result in the introduction of interstitial oxide ions to provide the charge compensation required in the  $\text{R}^{3+}$  doped  $\text{CdSiO}_3$ .

### 2.2. Synchrotron radiation UV-VUV spectroscopy

The UV-VUV excitation spectra of  $\text{CdSiO}_3$  were recorded between 80 and 330 nm using the SUPERLUMI (beamline I) synchrotron radiation facility of HASYLAB (Hamburger Synchrotronstrahlungslabor) at DESY (Deutsches Elektronen-Synchrotron, Hamburg, Germany) [10]. The polycrystalline materials were mounted on the cold finger of a liquid He flow cryostat and the spectra were recorded at 10 K. The setup consisted of a 2 m McPherson-type primary (excitation) monochromator with a resolution up to 0.02 nm. The UV-VUV excitation spectra were corrected for

the variation in the incident flux of the excitation beam using the excitation spectrum of sodium salicylate as a standard.

### 2.3. Calculation method

The electronic structures of the pure and interstitial oxide containing  $\text{CdSiO}_3$  were calculated employing the density functional theory with the WIEN2k package [11]. WIEN2k is based on the full potential linearized augmented plane wave method (LAPW), an approach which is among the most precise and reliable ways to calculate the electronic structure of solids. The semi-local spin density generalized gradient approximation (GGA) method was applied.

One interstitial oxide ion ( $\text{O}_i^{2-}$  with a double negative net charge) was introduced in the normal unit cell of  $\text{CdSiO}_3$  (Z: 4 [9]), including thus 60 atoms without  $\text{O}_i^{2-}$ . A detailed description of the  $\text{CdSiO}_3$  structure is given in section 3.1.1. The reliable calculation of the electronic structure requires the optimization of the crystal structure. This was achieved by relaxing the positions of all atoms in the unit cell, while the lattice parameters were not changed. No major modifications in the lattice parameters are expected due to  $\text{O}_i^{2-}$ , but these parameters too will be optimized in the further studies. In the DFT calculations, the single particle Kohn-Sham equations can be solved on a grid of sampling points ( $k$ -points) in the symmetry irreducible wedge of the Brillouin zone [12]. The number of the  $k$ -points in the irreducible part of the Brillouin zone of  $\text{CdSiO}_3$  was 8 and 20 for the pure and  $\text{O}_i^{2-}$  containing host, respectively. The number of basis functions used was *ca.* 6500.

## 3. Results and discussion

### 3.1. Structure optimization

#### 3.1.1. Crystal structure

The  $\text{CdSiO}_3$  materials possess the monoclinic structure (space group:  $P2_1/c$ , no. 14, Z: 4, a: 6.9463, b: 7.2563, c: 15.0700 Å and  $\beta$ : 94.791° [9]) with three Cd and Si as well as nine O sites. The structure contains distorted  $\text{CdO}_6$  octahedra which are arranged in slabs parallel to [010]. Three such slabs constitute ribbons which are separated from each other by unbranched dreier single chains with three  $\text{SiO}_4$  tetrahedra in the repeat unit (Fig. 1). The overall three-fold symmetry gives a systematic  $\text{Cd}_3[\text{Si}_3\text{O}_9]$  formula, however, the formula  $\text{CdSiO}_3$  is used in this work for the sake of simplicity.

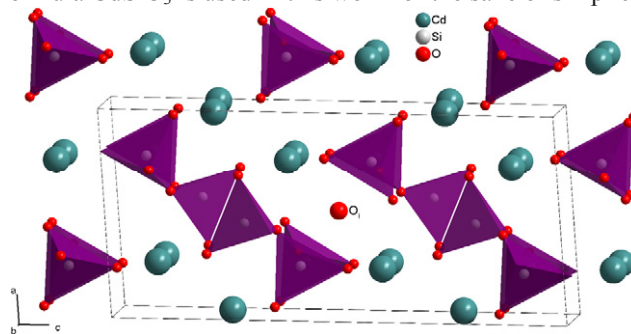


Fig. 1. The original monoclinic structure (space group  $P2_1/c$ ) of  $\text{CdSiO}_3$  with an interstitial oxide ion in the  $(\frac{1}{2}, \frac{1}{2}, \frac{1}{2})$  site (figure prepared with DIAMOND [13] with structural data from [9]).

A free space for the possible accommodation of the interstitial oxide ion is found in the 2b ( $\frac{1}{2}, \frac{1}{2}, \frac{1}{2}$ ) site (Fig. 1). The Cd-Cd distance between the terminal Cd belonging to different ribbons on each side of this site is *ca.* 5.2 Å whilst rather short distances of *ca.* 3.4 Å are found within the ribbons composed of three CdO<sub>6</sub> octahedra. The shortest O<sub>i</sub><sup>''</sup>-O<sub>i</sub><sup>''</sup> distance is 6.9 Å (along the a axis) between different unit cells. The interstitial ion can be considered isolated despite this rather short distance and the local changes in the crystal and electronic structure induced by it may be probed. The feasibility of the introduction of the interstitial defect is discussed in detail in the following sections.

### 3.1.2. Structural modifications due to an interstitial oxide

O<sub>i</sub><sup>''</sup> stays very close to the ( $\frac{1}{2}, \frac{1}{2}, \frac{1}{2}$ ) site even with structure optimization using DFT. Only an insignificant shift of 0.011 Å along the unit cell ab plane was found (Table). In contrast, the nearest oxygen atoms (O4 site) and the closest Cd<sup>2+</sup> ions (Cd3 and Cd2) move towards O<sub>i</sub><sup>''</sup>, whereas most of the other atoms near this defect move away from it. The most significant distortions in the unit cell take place within *ca.* 3.6 Å distance from O<sub>i</sub><sup>''</sup> (atoms within this distance are indicated in Table 1.).

Table 1. Atomic positions and distances (up to 3.6 Å) of the nearest atoms to the interstitial oxide ion in the original and optimized crystal structure of CdSiO<sub>3</sub> (distances and differences in Å).

Species	Original			Distance <sup>a</sup>	Optimized			Distance <sup>a</sup>	Difference <sup>b</sup>
	x	y	z		x	y	z		
O <sub>i</sub> <sup>''</sup>	0.5000	0.5000	0.5000		0.5012	0.4992	0.5000		
O4a	0.7686	0.3711	0.4852	2.115	0.7400	0.3668	0.4906	1.932	-0.183
O4b	0.2314	0.6289	0.5148		0.2598	0.6329	0.5095	1.953	-0.162
O5a	0.7023	0.6239	0.5996	2.164	0.7588	0.6365	0.6179	2.612	0.448
O5b	0.2977	0.3761	0.4004		0.2414	0.3637	0.3822	2.616	0.452
Si2a	0.7606	0.4098	0.5894	2.261	0.7648	0.4171	0.5974	2.327	0.066
Si2b	0.2394	0.5902	0.4106		0.2349	0.5830	0.4028	2.342	0.081
O8a	0.5842	0.3018	0.6333	2.450	0.6029	0.3195	0.6557	2.725	0.275
O8b	0.4158	0.6982	0.3667		0.3969	0.6807	0.3444	2.732	0.282
Cd3a	0.7463	0.6199	0.3985	2.542	0.7227	0.6275	0.3983	2.444	-0.098
Cd3b	0.2537	0.3801	0.6015		0.2772	0.3727	0.6016	2.451	-0.091
Si1a	0.7615	0.8388	0.5899	3.281	0.7813	0.8534	0.5918	3.443	0.162
Si1b	0.2385	0.1612	0.4101		0.2187	0.1469	0.4082	3.442	0.161
O3a	0.2259	0.1201	0.5132	3.366	0.2413	0.1192	0.5139	3.312	-0.054
O3b	0.7741	0.8799	0.4868		0.7585	0.8808	0.4861	3.312	-0.054
Cd2a	0.7504	0.1279	0.4013	3.600	0.7224	0.1245	0.3978	3.538	-0.062
Cd2b	0.2496	0.8721	0.5987		0.2776	0.8753	0.6020	3.553	-0.047

<sup>a</sup> Distance to O<sub>i</sub><sup>''</sup>.

<sup>b</sup> Difference to the distance in the original (non-optimized) structure.

The introduction of O<sub>i</sub><sup>''</sup> induced tilting of the SiO<sub>4</sub> groups (Fig. 2) which is indicated by the modifications in the O<sub>i</sub><sup>''</sup>-O distances (Table). The shortest O<sub>i</sub><sup>''</sup>-O4 ones were decreased by *ca.* 0.17 Å relative to the original value due to the structure optimization. These distances (1.93-1.95 Å) are clearly shorter than the O-O distance in the SiO<sub>4</sub> tetrahedra (2.54-2.80 Å) in CdSiO<sub>3</sub> which indicates significant structural strains. The pronounced electrostatic repulsion between O<sub>i</sub><sup>''</sup> and atoms in the O4 site may reduce the stability of the interstitial oxide though the bonding characteristics of these two species are different. The stability of O<sub>i</sub><sup>''</sup> may be further reduced by the strong increase (by 0.45 Å, Table) in the O<sub>i</sub><sup>''</sup>-O5 distances – originally almost similar to O<sub>i</sub><sup>''</sup>-O4. Such strong distortions in the local environment of O<sub>i</sub><sup>''</sup> may lead to its removal from the CdSiO<sub>3</sub> structure. The interstitial oxide might in this case be replaced by trapped electrons to conserve the charge compensation in the case of eventual R<sup>3+</sup> doping. This trap could

play an important role in persistent luminescence since electrons were shown to act as charge carriers in  $\text{CdSiO}_3:\text{Tb}^{3+}$  [5]. However, these trapped electrons cannot be probed using the current DFT method. Their presence should be confirmed by other means, using *e.g.* the electron paramagnetic resonance (EPR) spectroscopy.

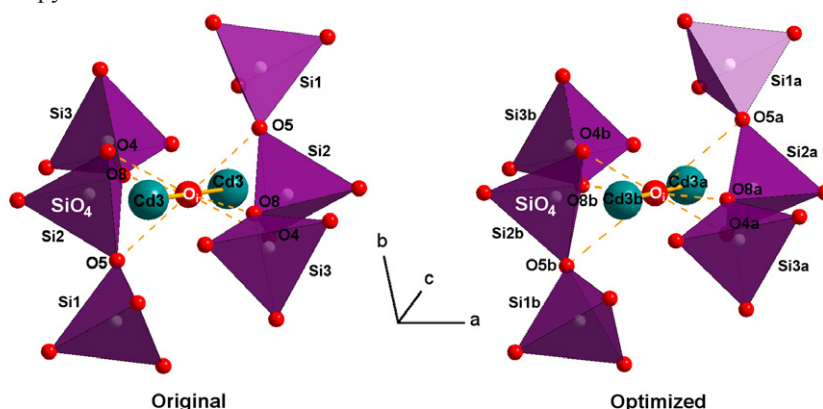


Fig. 2. Environment of the interstitial oxide ion in the original ( $\frac{1}{2}, \frac{1}{2}, \frac{1}{2}$ ) site (left) and in the structure optimized (right)  $\text{CdSiO}_3$ .

The  $\text{O}_i^{\bullet-}$ -Cd distances were slightly decreased due to the DFT structure optimization, whereas  $\text{O}_i^{\bullet-}$ -Si were increased (Table and Fig. 2). The optimized  $\text{O}_i^{\bullet-}$ -Cd3 distances of *ca.* 2.45 Å are a little longer than the optimal R-O bond distance (2.30 Å calculated from the ionic radii [7] for  $\text{Tb}^{3+}$  and  $\text{O}^{2-}$ ) but well within the range found in reality for the R-O bond. Therefore, the formation of a  $\text{R}_{\text{Cd}}^{\bullet+}-\text{O}_i^{\bullet-}-\text{R}_{\text{Cd}}^{\bullet+}$  defect cluster should be considered probable in  $\text{CdSiO}_3$ . The introduction of  $\text{R}_{\text{Cd}}^{\bullet+}$  in the local environment of the interstitial oxide should shift some of the electron density from  $\text{O}_i^{\bullet-}$  towards the positively charged  $\text{R}_{\text{Cd}}^{\bullet+}$ . The electrostatic repulsion of  $\text{O}_i^{\bullet-}$  and nearest oxygen atoms is thus decreased which increases the stability of the interstitial defect.

The calculated total energy (*ca.* -1998 keV) of the  $\text{O}_i^{\bullet-}$  containing  $\text{CdSiO}_3$  was decreased by 2 eV due to the structure optimization despite the rather significant distortions induced by  $\text{O}_i^{\bullet-}$ . The decrease – although only minor – in the total energy indicates the flexibility of the  $\text{CdSiO}_3$  structure which allows the modifications in the local environment of the defect. In reality, this is shown by the different polymorphs of  $\text{CdSiO}_3$  (or  $\text{CaSiO}_3$ ). Therefore, the introduction of an interstitial oxide ion in  $\text{CdSiO}_3$  should not be ruled out and the electronic structure of the pure and defect containing material is discussed in the following sections.

### 3.2. Electronic structure

#### 3.2.1. Host band structure

The electronic band structure along a high symmetry path in the first Brillouin zone (BZ) as well as the density of states (DOS) of the monoclinic  $\text{CdSiO}_3$  was calculated as the starting point of the DFT studies (Fig. 3). The minimum of the conduction band is located at the origin of BZ (K1 in Fig. 3) at 3.0 eV above the maximum of the valence band, though the density of states is low at this energy. The maximum of VB does not occur at this point which indicates an indirect band gap. However, the difference between

the top of VB (between K3 and K4) and energy at the origin of BZ (K1) is only 0.05 eV. The valence band has mainly the O 2p character with a pronounced Cd 4d character 5.3-6.5 eV below the top of VB (Fig. 4). The conduction band consists mostly of Cd (5s and 5p, 5.1+ eV) and Si (3p, 8+ eV) levels.

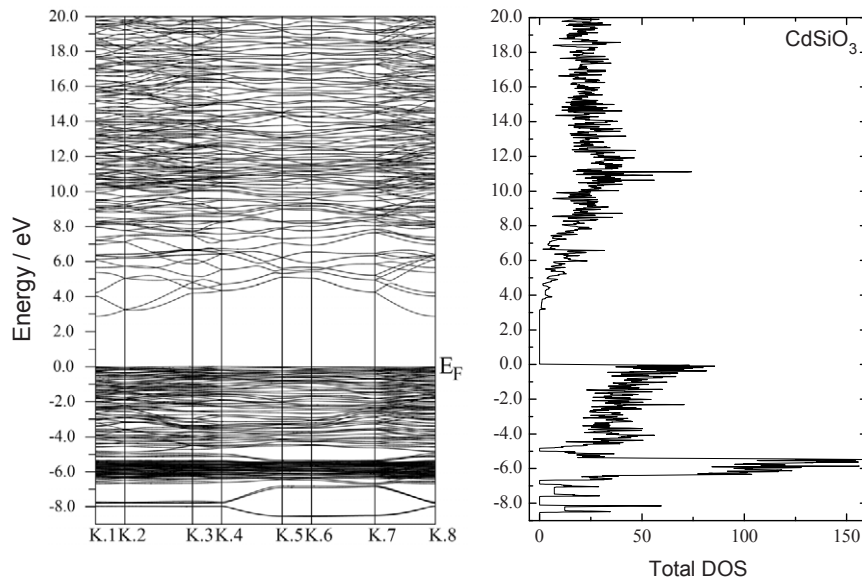


Fig. 3. Calculated (GGA method) band structure along a high symmetry path in the first Brillouin zone (left;  $E_F$ : Fermi energy) and total density of states of  $\text{CdSiO}_3$  (right).

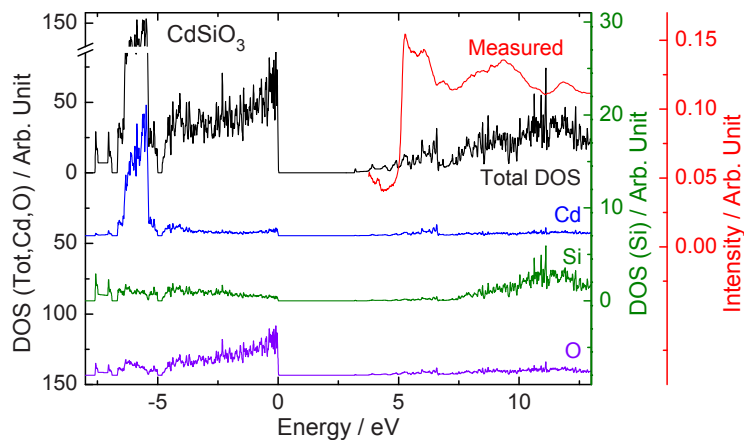


Fig. 4. Calculated (GGA method) density of states with the UV-VUV synchrotron radiation excitation spectrum of  $\text{CdSiO}_3$  at 10 K ( $\lambda_{em}$ : 600 nm).

The DFT calculations did not provide an absolute measure for the band gap energy ( $E_g$ ) due to the presence of non-zero DOS 3.0-4.9 eV situated above the top of the valence band (Figs. 3 and 4). This might suggest the presence of intrinsic shallow electron traps which exist even without the introduction of

any defects in CdSiO<sub>3</sub>. It is possible that these traps are, in fact, due to the empty space in the structure around the normally vacant (1/2, 1/2, 1/2) site. A more significant increase in the DOS appears at 5.1 eV which may be used as a more reliable measure for E<sub>g</sub> than the scattered DOS at lower energy.

Derivatives of both the calculated total DOS and synchrotron radiation excitation spectrum of the non-doped CdSiO<sub>3</sub> material were used to obtain accurate and comparable E<sub>g</sub> values. A perfect agreement between the experimental and calculated values (5.1 eV for both) was thus found. The relatively low band gap energy of CdSiO<sub>3</sub> is required to obtain persistent luminescence from the Tb<sup>3+</sup> doped material using low energy UV irradiation since the <sup>7</sup>F<sub>6</sub> ground levels of Tb<sup>3+</sup> are considerably farther below the CB of the host than the <sup>8</sup>S<sub>7/2</sub> ground level of Eu<sup>2+</sup> [5]. The present results represent a significant improvement on the previously reported discrepancy of *ca.* 2.5 eV between the experimental and calculated E<sub>g</sub> of triclinic CdSiO<sub>3</sub> [8].

### 3.2.2. Interstitial oxide containing material

The structure of the valence and conduction bands as well as the E<sub>g</sub> value did not change to any significant extent from the pure to the O<sub>i</sub><sup>••</sup> containing CdSiO<sub>3</sub> (Fig. 5). In addition, no changes in the host band structure resulted from the structure optimization despite the rather significant modifications caused by the introduction of the interstitial defect. Scattered DOS 3.2-4.9 eV situated above the top of VB (*cf.* section 3.2.1.), possibly corresponding to shallow electron traps, is found also for this defect containing material. Thus the introduction of O<sub>i</sub><sup>••</sup> does not modify the electronic structure close to the conduction band which could affect the thermally controlled bleaching of electron traps involved in the persistent luminescence mechanism [5].

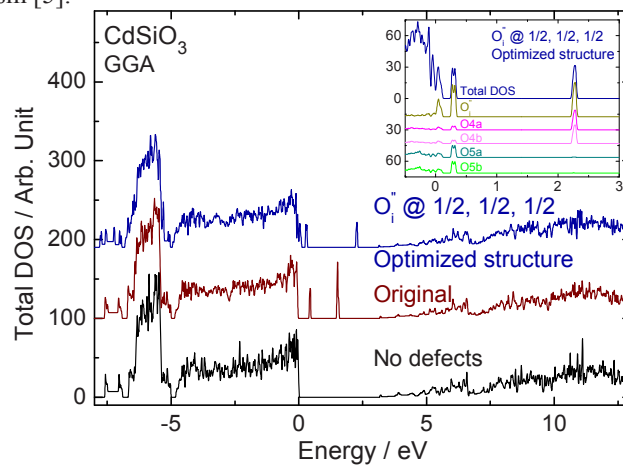


Fig. 5. Calculated (GGA method) density of states of the original and structure optimized CdSiO<sub>3</sub> with and without an interstitial oxide ion. Inset: Calculated total density and partial density of O<sub>i</sub><sup>••</sup> and oxygen atoms in the O4 and O5 sites.

Defect levels are created at 0.45 and 1.52 eV above the top of VB with the introduction of the interstitial oxide (Fig. 5, original structure). The level at higher energy has O 2p character from O<sub>i</sub><sup>••</sup> and the nearest two oxygens (the O4 site) of the SiO<sub>4</sub> groups. The defect level is created in the forbidden band due to the pronounced electrostatic repulsion between these species (*cf.* section 3.1.2.). With structure optimization, this level shifts by 0.76 eV to higher energy due to the increased electron repulsion which is induced by the very short O<sub>i</sub><sup>••</sup>-O4 distances. Such a defect level is unlikely to act as an electron trap due to

the strong electrostatic repulsion. In any case, the possible electron trap created by this defect level is too deep (2.82 eV below CB) to be bleached at room temperature.

The occupied defect level at lower energy has O 2p character from O<sub>1</sub><sup>''</sup> and the two next nearest oxygens (the O5 site, Fig. 5) with some character also from the O4 site. This level shifts by 0.18 eV to lower energy due to the significant increase (Table) in the O<sub>1</sub><sup>''</sup>-O5 distances with structure optimization. The electrostatic repulsion is thus decreased which lowers the energy position of the defect level and leads to the creation of a possible shallow hole trap only 0.27 eV above the top of VB. However, hole traps are not expected to be involved in Tb<sup>3+</sup> persistent luminescence.

Vacancies can also create traps which act as the energy storage sites in CdSiO<sub>3</sub>. Efficient trapping of electrons by oxygen vacancies as well as the role of cation vacancies as hole traps was indicated recently in the Sr<sub>2</sub>MgSi<sub>2</sub>O<sub>7</sub> host [14,15]. In addition, aggregation of the defects with the adjacent R<sup>3+</sup> ions is expected to modify the trap depths. These effects including a detailed study of the electronic structure of CdSiO<sub>3</sub>:R<sup>3+</sup> will be the subject of a further work.

#### 4. Conclusions

The introduction of an interstitial oxide ion provides a convenient charge compensation scheme required by the R<sup>3+</sup> doping in CdSiO<sub>3</sub>. However, the crystal structure of CdSiO<sub>3</sub> was significantly modified due to this defect when optimized with DFT calculations. Very short distances to the nearest oxygen atoms result in pronounced electrostatic repulsion. This may induce the removal of the interstitial oxide and possible formation of an electron trap in the defect site. However, the optimized Cd-O distances correspond well to the regular R-O ones and the eventual R<sup>3+</sup> doping is expected to increase the stability of this interstitial defect.

The experimental band gap energy was perfectly reproduced by the calculations. Intrinsic electron traps were indicated even without the introduction of structural defects and they may have a role in the energy storage in CdSiO<sub>3</sub>. Possible electron and hole traps were found in the interstitial oxide ion containing host, though the electron traps are too deep to allow release at room temperature which is a requirement for persistent luminescence. The R<sup>3+</sup> energy level positions *vis-à-vis* the CdSiO<sub>3</sub> host band structure as well as the modification of the defect energy levels due to the defect aggregation are worth separate studies. The trap levels induced by vacancies should also be determined since they are expected to affect the persistent luminescence efficiency of this material.

#### Acknowledgements

Financial support is acknowledged from the Turku University Foundation, Jenny and Antti Wihuri Foundation (Finland) and the Academy of Finland (contracts #123976/2006, #134459/2009 and #137333/2010). The DFT calculations were carried out using the supercomputing resources of the CSC IT Center for Science (Espoo, Finland). The study was supported by research mobility agreements (112816/2006/JH and 116142/2006/JH, 123976/2007/TL) between the Academy of Finland and the Academy of Sciences of the Czech Republic as well as the Czech research project AVOZ10100521 (PN). The synchrotron radiation study was supported by the European Community's Seventh Framework Programme (FP7/2007-2013) under grant agreement n° 312284. Dr. Aleksei Kotlov (HASYLAB) is gratefully acknowledged for his assistance during the synchrotron measurements. The financial support from CNPq, Nanobiotec-Brasil RH-INAMI, inct-INAMI, FAPESP, Coimbra Group and CAPES (Brazil) is gratefully acknowledged, too.

## References

- [1] Brito HF, Hölsä J, Jungner H, Laamanen T, Lastusaari M, Malkamäki M, Rodrigues LCV. Persistent luminescence fading in  $\text{Sr}_2\text{MgSi}_2\text{O}_7:\text{Eu}^{2+},\text{R}^{3+}$  materials: A thermoluminescence study. *Opt. Mater. Expr.* 2012;**2**:287-93.
- [2] Aitasalo T, Hölsä J, Jungner H, Lastusaari M, Niittykoski J. Thermoluminescence study of persistent luminescence materials:  $\text{Eu}^{2+}$ - and  $\text{R}^{3+}$ -doped calcium aluminates,  $\text{CaAl}_2\text{O}_4:\text{Eu}^{2+},\text{R}^{3+}$ . *J. Phys. Chem. B* 2006;**110**:4589–98.
- [3] Lin Y, Tang Z, Zhang Z, Nan CW. Anomalous luminescence in  $\text{Sr}_4\text{Al}_{14}\text{O}_{25}:\text{Eu},\text{Dy}$  phosphors. *Appl. Phys. Lett.* 2002;**81**:996-8.
- [4] Lin Y, Tang Z, Zhang Z, Wang X, Zhang J. Preparation of a new long afterglow blue-emitting  $\text{Sr}_2\text{MgSi}_2\text{O}_7$ -based photoluminescent phosphor. *J. Mater. Sci. Lett.* 2001;**20**:1505-6.
- [5] Rodrigues LCV, Brito HF, Hölsä J, Stefani R, Felinto MCFC, Lastusaari M, Laamanen T, Nunes LAO. Discovery of the persistent luminescence mechanism of  $\text{CdSiO}_3:\text{Tb}^{3+}$ . *J. Phys. Chem. C* 2012;**116**:11232-40.
- [6] Kröger FA, Vink HJ. *Semiconductors and phosphors*. Proc. Intern. Colloq.: Garmisch-Partenkirchen, Germany; 1958; p 17.
- [7] Shannon RD. Revised effective ionic radii and systematic studies of interatomic distances in halides and chalcogenides. *Acta Cryst. A* 1976;**32**:751-67.
- [8] Barboza CA, Henriques JM, Albuquerque EL, Freire VN, da Costa JAP, Caetano EWS. Triclinic  $\text{CdSiO}_3$  structural, electronic, and optical properties from first principles calculations. *J. Phys. D: Appl. Phys.* 2009;**42**:155406-1-8.
- [9] Weil M. Parawollastonite-type  $\text{Cd}_3[\text{Si}_3\text{O}_9]$ . *Acta Cryst. E* 2005;**61**:i102-4.
- [10] Beamline I (SUPERLUMI) Home Page. [http://hasylab.desy.de/facilities/doris\\_iii/beamlines/i\\_superlumi](http://hasylab.desy.de/facilities/doris_iii/beamlines/i_superlumi) (accessed on June 18, 2012).
- [11] Blaha P, Schwarz K, Madsen GKH, Kvasnicka D, Luitz J. *WIEN2k, An augmented plane wave + local orbitals program for calculating crystal properties*. Schwarz K-H, Technische Universität, Wien, Austria; 2001 (ISBN 3-9501031-1-2).
- [12] Singh DJ. *Planewaves, pseudopotentials and the LAPW method*. Kluwer: Norwell, MA, USA; 1994, p. 5-9.
- [13] Brandenburg K. *Diamond*, v.3.2g; Crystal Impact: Bonn, Germany; 2011.
- [14] Hassinen J, Hölsä J, Laamanen T, Lastusaari M, Novák P. Electronic structure of defects in  $\text{Sr}_2\text{MgSi}_2\text{O}_7:\text{Eu}^{2+},\text{La}^{3+}$  persistent luminescence material. *J. Non-Cryst. Solids* 2010;**356**:2015-9.
- [15] Hölsä J, Laamanen T, Lastusaari M, Novák P. Defect aggregates in the  $\text{Sr}_2\text{MgSi}_2\text{O}_7$  persistent luminescence material. *J. Rare Earths* 2011;**29**:1130-6.